

Energetics of K^+ permeability through Gramicidin A by forward-reverse steered molecular dynamics

G. De Fabritiis,^{1,*} P. V. Coveney,^{2,†} and J. Villà-Freixa^{1,‡}

¹*Computational Biochemistry and Biophysics Laboratory (GRIB-IMIM), Universitat Pompeu Fabra, Barcelona Biomedical Research Park, C/ Dr Aiguader 88, 08003 Barcelona, Spain.*

²*Centre for Computational Science, Department of Chemistry, University College London, 20 Gordon Street, WC1H 0AJ London, United Kingdom.*

The estimation of ion channel permeability poses a considerable challenge for computer simulations due to the significant free energy barriers involved, but also offers valuable molecular information on the ion permeation process not directly available from experiments. In this paper we determine the equilibrium free energy barrier for potassium ion permeability in Gramicidin A in an efficient way by atomistic forward-reverse non-equilibrium steered molecular dynamics simulations, opening the way for its use in more complex biochemical systems. Our results indicate that the tent-shaped energetics of translocation of K^+ ions in Gramicidin A is dictated by the different polarization responses to the ion of the external bulk water and the less polar environment of the membrane.

Keywords: steered molecular dynamics, Crooks fluctuation relation, Gramicidin A, ion permeation, potential of mean force

I. INTRODUCTION

In recent years, the three dimensional structures of an increasing number of membrane transport proteins have been solved (see refs. in [1]). This, among other advances, has led to a better understanding of some important examples including the mechanisms of channel blocking by small molecules, as occurs in the drug-induced long QT syndrome [2] caused by the blocking of the hERG K^+ channel; the study of conformational changes affecting channel gating [3]; the understanding of the selectivity for specific ions [4]; and the evaluation of ion conductivity [5]. Furthermore, a revolution in the development and application of computational techniques to unravel structure-function relationships in these systems has been triggered (for reviews, see [6–9]). However, for the case of conductivity of ions and water molecules through membrane proteins, the computational elucidation of the underlying factors affecting the energetics of the ions within the channel remains a major challenge for current molecular simulation techniques. The reason for this resides in the long time scales for these processes (which are of the order of milliseconds).

The use of simulation techniques to understand the microscopic behavior of ion channels is challenging because the ions have to surmount considerable free energy barriers. The evaluation of such free energy barriers presents the modeler with a twofold difficulty: the need for an accurate description of the electrostatics of the pore which can be achieved by full-atom simulations, and the requirement to sample efficaciously highly improbable, high energy regions, of the potential energy surface.

Nevertheless, a proper characterization of the energetics of the ion-protein interaction is critical for obtaining high quality results. Full atomistic simulations have been used with some success on ion selectivity studies [10–14], although it has been pointed out that a proper treatment of ion selectivity would necessarily imply the extremely challenging characterisation of the absolute free energies of ion crossing, that ultimately may lead to differences in ion current between different ionic species[15]). In addition, full atomistic representations are less suitable for simulating long time scale processes and to this end methods with typically lower resolution of the energetic properties within the channel are then selected to describe the ion movement [15, 16]. It is because of this problem that most studies are built on a two step protocol for analyzing the dynamics of the ions. First, the effective potential experienced by the ion within the channel is computed by means of a potential of mean force (PMF) calculated with some sort of histogram method [17] or by single ion solvation calculations performed across the channel [16, 18]. Second, the dynamics of the ions under this effective potential is evaluated by some sort of stochastic simulation protocol. In this paper we are concerned about the first aspect: the application of a technique that efficiently samples the high energy regions while retaining the precise atomistic description of the system for the protein, membrane and solvent.

Until the recent solution of the KcsA K^+ and the MscL X-ray structures [19, 20], the availability of structural information on protein channels was limited to that of the Gramicidin A (gA) peptide, which indeed led to some of the first computational studies in the field [21, 22]. gA (see Figure 1) is a helical antibacterial pentadecapeptide with alternating D- and L- amino acids used to increase the permeability of biological membranes to inorganic ions, and it is often used in combination with other drugs to increase their effectiveness [23]. The pore formed by gA is one of the most studied both biochemically and

*gianni.defabritiis@upf.edu

†p.v.coveney@ucl.ac.uk

‡jvilla@imim.es

structurally by means of a number of computer simulations [24, 25]. Surprisingly, permeation for this simple pore is less well characterized [26–28] than for other larger and more complex membrane proteins ([13, 16, 29]). The discrepancy between experiment and simulation has been explained on various grounds such as lack of sampling, a poor force field in terms of polarization of water and possibly different structures of the pore itself (also crystallized on a joined double helices structure that appears to be much more stable and robust than the dimeric conformation [26]). One particularity of this protein is that it forms a narrow pore, only allowing a single file of water molecules (or potassium ions) to fill it. The pore is, however, very active in transporting different types of monovalent ions, being able to handle two potassium ions at the same time [30]. In addition, owing to the diameter of the pore, the transport of a single ion drags with it a column of six to nine water molecules in a single file. This fact adds an extra challenge for the simulation of the conductivity through gA, as compared with other channels with wider pores, in which water molecules can slip past each other[30].

In this paper, we use a novel technique which is based on the use of forward-reverse steered molecular dynamics simulations [31–33] to populate high energy regions of the potential energy surface, and on the use of the Crooks fluctuation relation [31, 33, 34] to obtain an estimate of the free energy barrier for ion crossing. This methodology differs from more traditional biasing techniques [35] like umbrella sampling [27, 28], which reconstruct the free energy profile from several equilibrium simulations one for each bias potential along a discretized reaction coordinate. Instead, Crooks fluctuation relation allows us to reconstruct the *equilibrium* free energy from a set of non-equilibrium molecular dynamics simulations. This formula was recently applied, together with the acceptance ratio method [36], to determine the experimental folding free energy in an RNA pulling experiment via optical tweezers [37]. Our approach benefits from the fact that the reaction coordinate along which the steered molecular dynamics protocol is applied is well approximated by the axis perpendicular to the membrane surface. The application of this technique to distributed computational infrastructures is also discussed. Our results show that the differential induced polarization between the water molecules at the entrance of the pore and the apolar membrane atoms at its interior is a major source of the free energy barrier the potassium ions need to surmount in this system.

Section II contains a brief summary of the methods employed in this work, Section III includes the numerical results obtained and concluding remarks and discussion are given in Section IV.

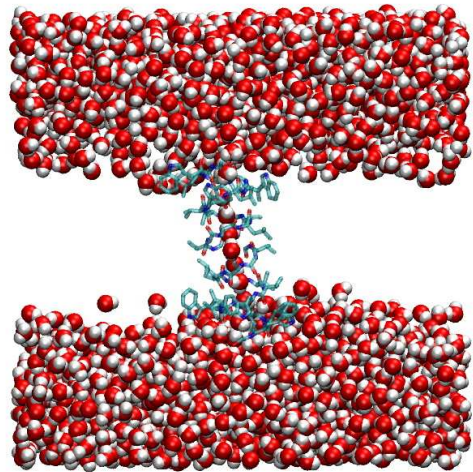


FIG. 1: The Gramicidin A pore solvated in a DMPC membrane, TIP3P water and 150mM KCl. A single column of water molecules is present inside the pore. Lipids are not shown for clarity.

II. METHODS

A. Potential of mean force

We start by defining a reaction coordinate $\xi = \xi(\mathbf{R})$ and the probability density of encountering any given value of this coordinate ξ' , given by the canonical ensemble average

$$\rho(\xi') = \frac{\int d\mathbf{R}d\mathbf{P}\delta(\xi(\mathbf{R}) - \xi') \exp(-\beta H)}{\int d\mathbf{R}d\mathbf{P} \exp(-\beta H)}, \quad (1)$$

where $H = H(\mathbf{R})$ is the Hamiltonian of the system, $\mathbf{R} = \mathbf{r}_1, \dots, \mathbf{r}_N$, $\mathbf{P} = \mathbf{p}_1, \dots, \mathbf{p}_N$ the atom positions and momenta respectively, N is the number of atoms, $\beta = 1/(k_B T)$, k_B is the Boltzmann constant, T the temperature of the system and δ the Dirac delta function. In the canonical ensemble, the free energy difference $\Delta A_{\xi_1 - \xi_0} = A(N, V, T, \xi_1) - A(N, V, T, \xi_0)$ between two states $\xi' = \xi_1$ and $\xi' = \xi_0$ is directly written in terms of $\rho(\xi')$ as

$$\Delta A_{\xi_1 - \xi_0} = -k_B T \log \frac{\rho(\xi_1)}{\rho(\xi_0)}. \quad (2)$$

This quantity is also called the potential of mean force (PMF), that is the free energy along a given generalized coordinate (reaction coordinate) ξ and written, up to an arbitrary constant, as $A(\xi) = -k_B T \log \rho(\xi)$. The PMF can be estimated directly from the density ρ in Eq. 2 [38, 39]. However, often the states at various values of ξ are scarcely populated and the logarithmic function is singular when $\rho(\xi)$ is close to zero; therefore special methods must be used in order to increase the sampling via a biasing protocol.

B. Non-equilibrium methods: forward reverse steered molecular dynamics

The importance of Crooks fluctuation relation resides in the fact that, given two systems “0” and “1” described by the Hamiltonians H_0 and H_1 , the equilibrium free energy difference between the two states ΔA can be recovered from [31, 34, 37]

$$\frac{P_F(+\beta W)}{P_R(-\beta W)} = \exp(\beta(W - \Delta A)), \quad (3)$$

where W is the external work done on the system by forcing it to change from state 0 to 1 and P_F, P_R are the probability distributions of releasing the work W into the system during a transformation in the forward (F) $0 \rightarrow 1$ and reverse (R) $1 \rightarrow 0$ direction respectively in a finite time τ .

The Crooks fluctuation relation is the most recent of set of methods which allow to compute the equilibrium free energy. It is a direct generalization of the Jarzynski equality (JE) [40]

$$\langle \exp(-\beta W) \rangle_F = \exp(-\beta \Delta A), \quad (4)$$

which is recovered from Crooks fluctuation relation by integrating both sides of Eq. 3. The exponential average in JE does not converge well, because the system rarely explores configurations associated with low work W which are the ones that contribute significantly to the integral. Due to these convergence problems, the JE (4) is typically used via a cumulant expansion [32]

$$A(\xi') \approx \langle W(t') \rangle_{\xi'} - \frac{\beta}{2} [\langle W(t')^2 \rangle_{\xi'} - \langle W(t') \rangle_{\xi'}^2], \quad (5)$$

where the ensemble average is performed over trajectories satisfying $\xi(\mathbf{R}(t')) = \xi'$.

It is also interesting in order to understand formula (3) to refer to its more common equilibrium counterparts often used for the calculation of the chemical potential. For an instantaneous transformation from state 0 to 1 (infinite force), the work W is given directly by $W = u = U_1 - U_0$, where U is the potential part of the Hamiltonian H and Eq. (3) coincides with an equilibrium relation previously derived by Shing and Gubbins [41], $\frac{P_F(u)}{P_R(-u)} = \exp(\beta(u - \Delta A))$. In this case, the forward process (F) corresponds to the insertion of an atom into a system of N atoms ($0 \rightarrow 1$), and the reverse process (R) to the deletion of an atom from a system of $N+1$ atoms ($1 \rightarrow 0$). In the same manner as for the JE and Crooks fluctuation relation, the Widom formula can be recovered [35] by integrating both sides of the Shing-Gubbins equation. Widom’s formula is used to compute the chemical potential by test particle insertion [39] and has well known poor convergence proprieties [42]. Most of the convergence problems associated with the Widom formula also apply to the JE, i.e. the exponential average hardly samples the importance region of the integral [33].

The Bennett acceptance ratio method [36] can be used to minimize the variance of the estimate in Eq. (3), also in conjunction with biasing protocols [42]. The derivation of the Bennett method for the Shing-Gubbins equation [41] applies with identical steps to the Crooks fluctuation relation

$$\exp(-\beta \Delta A) = \frac{\langle (1 + \exp(\beta W + C))^{-1} \rangle_F}{\langle (1 + \exp(\beta W - C))^{-1} \rangle_R} \exp(C), \quad (6)$$

with $C = -\beta \Delta A + \ln(n_F/n_R)$, where n_F and n_R are the number of samples for the F and R average. In practice, given that C depends on the result ΔA , this equation is solved self-consistently by choosing a reasonable starting value for C , e.g. $C = 0$.

In steered molecular dynamics (SMD) simulations the system is steered by applying an external force from an equilibrium state characterized by an initial reaction coordinate corresponding to the projection of a potassium ion on the z direction, $z = z(\mathbf{R}) = z_0$ to another state at $z = z_1$. The biased Hamiltonian is given by $H = H_0(\mathbf{R}) + V(\mathbf{R}, t)$, where the forcing potential is harmonic

$$V(\mathbf{R}, t) = \frac{k}{2} (z(\mathbf{R}) - z_0 - vt)^2, \quad (7)$$

$t = 0, \dots, \tau$ is the time required to traverse the coordinate from $z_0 = z(\mathbf{R}(0))$ to $z_1 = z(\mathbf{R}(\tau))$ and v the pulling speed. The pulling forces release a certain amount of work into the system

$$W(t) = \int_0^t dt' \frac{\partial V}{\partial t'}(z(\mathbf{R}(t')), t') = -k \int_0^t v dt' (z(\mathbf{R}(t')) - z_0 - vt'), \quad (8)$$

from which we subtract the instantaneous biasing potential [31] to obtain $\Delta W(t) = W(t) - V(\mathbf{R}_t, t)$.

In the protocol followed by Kosztin *et al.* [33] the PMF between the states can be obtained from the free energy difference of the biased system provided that the spring constant is strong $k > \max(\frac{2\alpha}{\delta z^2}, \frac{2U_{max}}{\delta z^2})$, where δz is the spatial resolution that we are seeking for the PMF, U_{max} is the maximum energetic barrier that we expect in δz and $\alpha \gg 1$. In the strong spring approximation, the free energy and dissipated work along the reaction coordinate can be computed using the Crooks fluctuation relation [33] by simply averaging the work associated with the forward and reverse paths:

$$\begin{aligned} \Delta A(z) &= (\langle \Delta W_z \rangle_F - \langle \Delta W_z \rangle_R) / 2, \\ \Delta W_d(z) &= (\langle \Delta W_z \rangle_F + \langle \Delta W_z \rangle_R) / 2, \end{aligned} \quad (9)$$

where W_d indicates the dissipative work and ΔW_z corresponds to the work computed by Eq. 8 along the trajectories satisfying the condition $z(R(t)) = z$, generated by pulling the ion along the forward path F from the entrance ($t = 0$) to the center of the Gramicidin pore ($t = \tau$) and *viceversa* from $t = \tau$ to $t = 0$ along the reverse path (R). Angular brackets denote averages which are taken over a set of repeated SMD simulations along

both forward and reverse paths. Note that the work definition in Eq. 8 is odd under time reversal.

Finally, assuming a linear dependence between the dissipative work and the position dependent frictional coefficient $\gamma(z)$ (Langevin type) of the K^+ ion, we can estimate the diffusion coefficient using the relation[33]

$$D(z) = \frac{k_B T}{\gamma(z)} = v \frac{\Delta z}{\beta \Delta W_d}, \quad (10)$$

where Δz is the length spanned by the reaction coordinate during the time τ .

C. An analytical model case

A comparison between the different non-equilibrium methods proposed is presented in this section using an analytical set-up which allows us to identify the PMF exactly. We have performed a one-dimensional Langevin simulation on a periodic line between -12 \AA and 12 \AA resembling the PMF barrier expected from Gramicidin A, with a height of approximately 12 kcal/mol (see Figure 2) using the potential

$$U_{PMF}(z) = B \cos\left(\frac{2\pi}{4L}z\right) + B/4 \cos\left(\frac{2\pi}{L/2}z\right), \quad (11)$$

where we have chosen $B = 10 \text{ kcal/mol}$ and $L = 12 \text{ \AA}$. The frictional coefficient is derived using $D = \frac{k_B T}{\gamma}$ with $D = 50 \text{ \AA}^2/\text{ns}$, temperature $T = 305 \text{ K}$ and the mass of the Langevin particle $m = 39.0983 \text{ g/mol}$ equivalent to that of the potassium ion.

Starting from the initial position $z_0 = -12 \text{ \AA}$, we have performed a set of 10 steered runs in the forward and 10 in the reverse directions with velocity $v = 10 \text{ \AA/ns}$ using the harmonic biasing potential given in Eq. 7. The work is computed using Eq. (8) and the free energy profile reconstructed using the Bennett method Eq. (6), the JE with cumulant expansion Eq. (5) and the forward-reverse method Eq. (9). The results shown in Figure (2)a indicate that the most accurate free energy profile is recovered by the forward-reverse method, at least for this simple system. The absolute errors shown in Figure (2)b show that the Bennett method seems to overestimate the profile more or less consistently across the domain, while the JE has a lot variability (a different set of 10 runs can significantly change the profile, for instance note the difference between the free energy computed with the forward and reverse runs). As a further check, in Figure (2)c we have computed the dissipative work for different values of the pulling speed v equal to 10, 20, 30 \AA/ns which demonstrates that for this simple system the linear dissipative force approximation (a property of the Langevin equation) is valid and therefore the diffusion coefficient can be computed using Eq. 10. The diffusion coefficient recovered from the simulations using Eq. (10) is $D = 49.5 \text{ \AA}^2/\text{ns}$, in very good agreement with the input diffusivity ($D = 50 \text{ \AA}^2/\text{ns}$). Results obtained from 100 runs are similar but have smaller errors.

It is probably not surprising that the JE cumulant expansion produces the least accurate results. Also, it can be expected that the forward-reverse method is more accurate than the Bennett method in this situation, even if the Bennett method is designed to reduce the variance of the estimate. In fact, the forward-reverse method uses the Crooks fluctuation relation (3) in the strong spring approximation. This implies that the forward and reverse distributions are Gaussians with the same variance, so that the formulas (9) are valid. As shown in Figure (2)d, the two distributions $P_F(W)$ and $P_R(W)$ satisfy this condition sufficiently for the spring constant used ($k = 10 \text{ kcal/mol/\AA}^2$). The Bennett acceptance ratio method does not use the strong spring approximation being merely a variance reduction formalism applied to a very slowly converging exponential average (Eq. 3). Furthermore, the smooth plots in Figure (2)d are generated with one thousand trajectories, while calculations on real systems are limited by the computational cost to tens drastically increasing the noise of the Bennett estimate.

D. Molecular modeling

The starting structure of the gA helical dimer was downloaded from the Protein Data Bank (PDB:1JNO) and embedded in dimyristoylphosphatidylcholine (DMPC) lipid bilayer using the scripting facilities of the VMD program [43]. The choice of this set up was motivated by the fact that it has provided good results in previous MD simulations[27]. The bilayer was set up with 64 lipids over a surface of dimensions $63 \times 63 \text{ \AA}^2$ based on the experimental cross-section of the DMPC lipid bilayer 61.7 \AA^2 . Four lipids were removed upon insertion of the protein, then the entire complex was solvated with TIP3P water and 150 mM KCl. The alignment of the protein with the membrane was such that the aromatic residues of tryptophan at the top and bottom would be roughly in the horizontal plane of the membrane (xy). The entire system of just over 29,000 atoms was first minimized with the protein fixed, then equilibrated with velocity re-initialization every 0.1 ps at 305 K for 5 ps and the protein restrained with a harmonic potential of 250 kcal/mol per atom. The pressure was equilibrated at 1 atm for 0.4 ns. The total volume after pressure equilibration was approximately $66 \times 66 \times 62 \text{ \AA}^3$. The backbone of the protein was then constrained with an harmonic potential of 5 kcal/mol, except for C-alpha atoms for which a force constant of 25 kcal/mol was used and progressively reduced to zero over 0.5 ns. A final 10 ns run of equilibration was performed and the last configuration taken for the production runs. The molecular dynamics simulations were performed using Charmm27[44] force fields as implemented in NAMD [45], PME electrostatics, rigid bonds and a time step of 2 fs. The protein was able to tilt and move in the membrane. The equilibrated structure

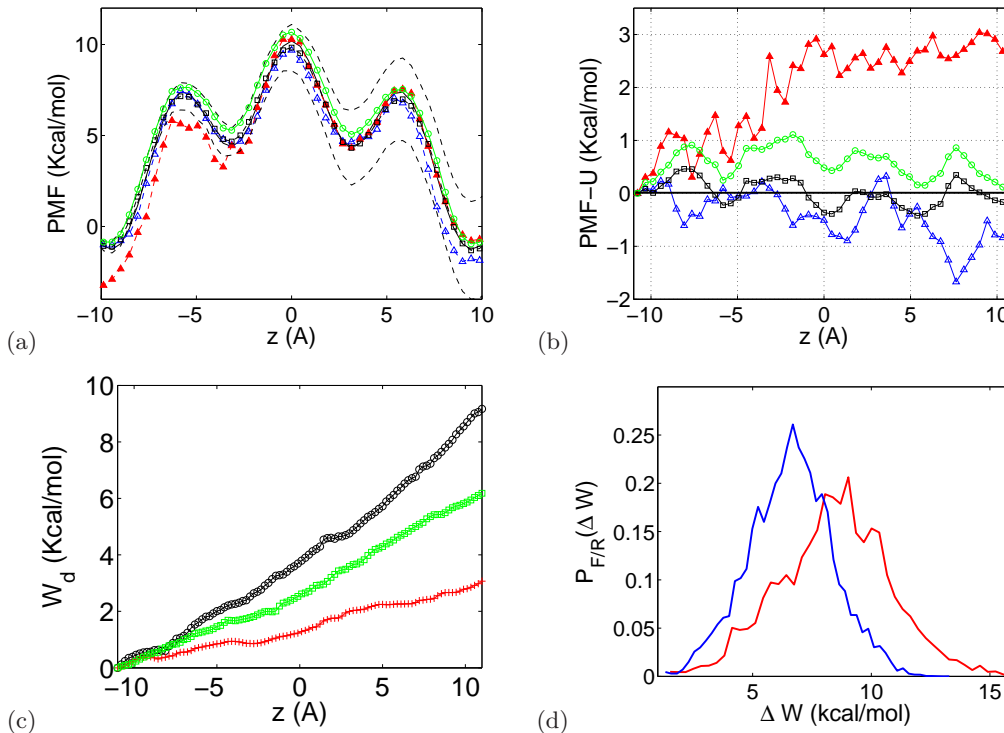


FIG. 2: (a) Application of different non-equilibrium methods for the reconstruction of the potential of mean force using Eq. 11 (solid black line). The profiles displayed are as follows: For the Jarzynski equation with cumulant correction Eq. (5), closed and open triangles for forward and reverse paths respectively; Bennett method Eq (6), open circles; forward-reverse SMD Eq. (9), open squares. All profiles are computed over 10 runs in each direction. Results from 100 runs are similar but with smaller errors. (b) The absolute error in the estimation of the PMF for all methods (same symbols as in (a)). (c) Scaling of the dissipative work for different pulling speeds v equal to 10 (plus signs), 20 (squares), 30 (circles) Å/ns. (d) Probability distribution of the work ΔW around one of the minima of Eq. 11 centered at $x = 3.2$ over a bin of 1 Å/ns and 1000 trajectories.

maintains a tilt of around 12 degrees with respect to the normal of the xy plane of the membrane (principal inertia axis of the C-alpha atoms is $(-0.218, -0.027, 0.975)$). The radius of the pore was estimated to be $r = 2.5$ Å by measuring the occupancy n_r of a water molecule at distance r from the pore central axis of symmetry, where r is the radius in cylindrical coordinates. The water occupancy along z (Fig. 3) is estimated directly from the MD trajectory by counting the average number of water molecules in cylindrical volumes of radius $r = 2.5$ Å and height $h = 1$ Å along the reaction coordinate.

E. Steered molecular dynamics simulations

Two sets of 25 of steered molecular simulations were performed where a K^+ ion was pulled along the z direction orthogonal to the pore from the pore entrance to the center (forward direction) and *viceversa* (reverse direction) taking advantage of the symmetry of the gA pore. The pulling speed is $v = 10$ Å/ns for 1.7 ns each run. The runs were performed within a NVT ensemble using Langevin dynamics with friction 1 ps^{-1} applied to the

system excluding hydrogen atoms and ions, a time step of 1 fs and a direct truncation cutoff of 12 Å. The forward runs start from an equilibrated structure with the K^+ ion located at the pore entrance. This equilibrated structure is selected from a 5 ns run during which a K^+ ion visited the binding site at the entrance of the channel (the ion remained in the site for tens of picoseconds only). The reverse runs simply start from a configuration with the ion at the center of the pore resulting from the last configuration of the forward runs equilibrated for 1 ns without any constraints.

Each run starts from the same equilibrated configuration but samples a different trajectory due to the random Langevin dynamics of the thermostat. The thermostat does not apply to the non-hydrogen atoms and to the ions in order to avoid affecting the diffusion (friction coefficient is $\gamma = 1 \text{ ps}^{-1}$). We also applied a harmonic restraining potential with $k = 250 \text{ kcal/mol } \text{Å}^{-2}$ to the center of mass of the C α s of the protein in order to avoid the possibility that the continuous strain on the surface of the pore produced by the pulled ion might affect the location of the protein in the membrane. With this setting the center of mass movement was limited to approx-

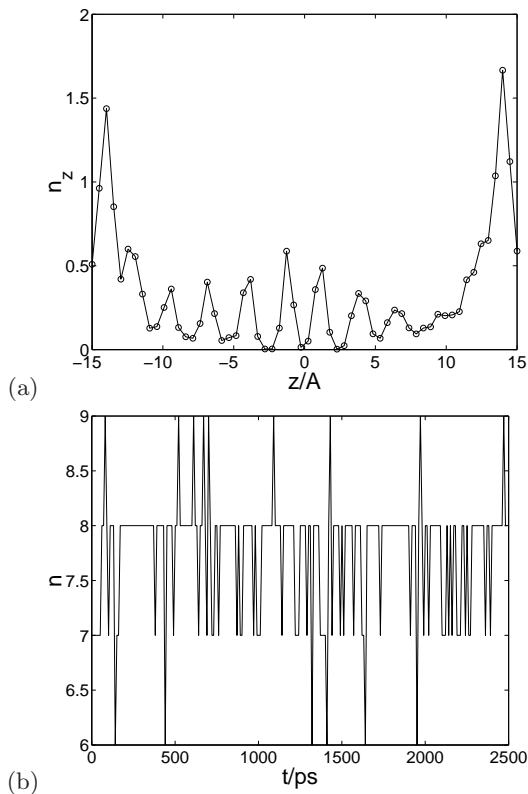


FIG. 3: Characterization of the water molecules present inside the pore. In a) is shown the water molecule occupancy n_z along the z direction of the pore. In b) the number of water molecules within 22 Å of the pore is plotted during a 2.5 ns simulation.

imately 0.1 Å. The reaction coordinate is always taken relative to the pore center of mass, in the z direction. From the 50 analyzed trajectories we have included the ones for which the water file inside the pore is not perfectly maintained during the simulation. In fact, for some trajectories, the pulled ion loses contact with the water behind it and the water molecule file inside the pore contains an empty position. In order to optimize the protocol, the pulling speed must be adjusted such that the single water file is maintained (low steering speed) while using the fastest possible speed in order to sample more trajectories. It is not clear *a priori* which pulling speed is best to use, but an extensive tuning of this parameter would be extremely costly. We have not found significant differences between the different pulling speeds $v = 10$ Å/ns and $v = 20$ Å/ns; nevertheless we have chosen to be on the safe side using the slower velocity.

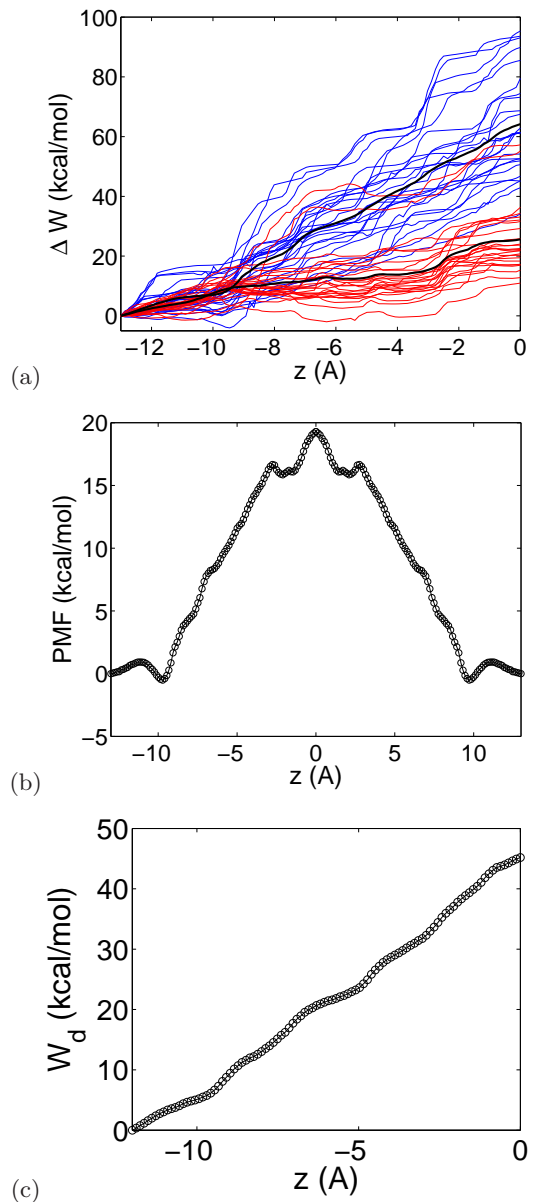


FIG. 4: (a) Work W_F and $-W_R$ obtained from Eq. 8 produced by pulling in the forward direction F (into the pore, continuous blue line) and reverse direction R (out of the pore, red line) a K^+ ion from -14 Å to the center of mass of the $C\alpha$ of gA. A set of 25 runs in each direction is performed. For convenience $-W_R$ is shifted to the origin at $z = -13$ Å. The average over the F and R runs are shown as thick solid lines. (b) The free energy profile reconstructed by Eq. 9 was made symmetric on the positive z axis. (c) Dissipated work performed on the ion within the pore obtained from Eq. 9.

III. RESULTS

A. Energetics of Gramicidin A

The work released to the system by the pulling is computed by a direct discretization of the integral of Eq. 8 over 100 bins. Each trajectory work data is divided into 50 bins over which the work and z position are time averaged. The resulting time series is used to compute the discrete integral [32]. The cumulative work performed across the pore is shown in Figure 4a for all forward and reverse pullings together with the average over forward and reverse runs separately. From these work paths, using Eq. 9 we computed the equilibrium free energy and the dissipated work directly. The reconstructed free energy profile is shown in Figure 4b. The energetic free energy barrier across the pore is approximately 19 kcal/mol with a binding site at the entrance to the pore at approximately -9.5 Å. Previous studies at the same ionic concentration of 150 mM KCl but using different simulation protocols and temperature (298K) [46] obtained a free energy barrier of approximately 15 kcal/mol. Another more recent study [28], at the same ion concentration and temperature as these calculations, found a barrier of approximately 13 kcal/mol from the entrance binding site, but at much higher ionic concentrations (1 M KCl) [27] the energetic barrier was also measured at 10 kcal/mol. All these different results are in disagreement with the experimental value of the conductance and confirm the difficulty of modeling this narrow channel by computational means. A comparison of the PMF produced by our SMD experiments and recent results [46] using the WHAM [47] and TI [35] methods for the same system with a similar setup is illustrative of the SMD methodology. In that study [46], the PMF is reconstructed between -20 and 20 Å, while we limit our domain to the range where the channel is considered narrow and uni-dimensional (-13 Å and 13 Å). This is to guarantee that the uni-dimensional approximation for the reaction coordinate z is still valid. Indeed, outside the channel the volume of the configurational space in the x, y direction will vary until reaching the bulk. A restraining potential is therefore required to maintain the ion constrained and aligned as if is in the pore, effectively extending the pore within the bulk domain. This potential needs then to be corrected with the two dimensional PMF[27]. Comparing the profiles in [46] with Fig. 4, it transpires that the two PMFs are similar in terms of the total barrier from the external ion binding site, as well as regarding the shape at the center. The depth of the binding site is however much smaller on our PMF without restraints probably due to the extended volume of space which the ion encounters at the boundary between the channel and the bulk.

The diffusion coefficient of K^+ ions is constant across the pore (linear slope of the dissipated work in Fig. 4c). The resulting value is computed using Eq. 10, giving $D = 1.75 \text{Å}^2/ns$ which is of the same order of magnitude

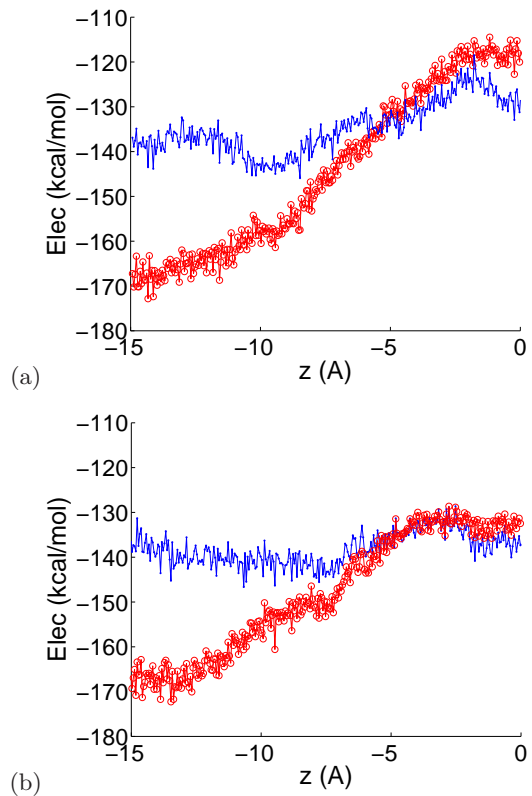


FIG. 5: Electrostatic interaction energy averaged over the forward (a) and reverse (b) pullings on all atoms within a sphere of radius 6 Å (dots) and 16 Å (circles) centered on the crossing ion.

as other numerical studies [48]. As a comparison, the approximate diffusion coefficient of K^+ ions in bulk water is $D = 190 \text{Å}^2/ns$ [48] and the self-diffusion of water is $D = 250 \text{Å}^2/ns$, two orders of magnitude higher. The higher diffusion coefficient of K^+ in bulk water is due to the fact that, in the pore, the ion binds electrostatically with oxygen atoms within the backbone of Gramicidin A inside the pore. These binding sites are very stable, reducing significantly the diffusivity of the ion compared to bulk water. Overall, the relation Eq. 10 is valid only if we can assume a linear dependence of the dissipative work with the pulling velocity. This assumption is verified in the simple Langevin case of section II C, however preliminary runs at different pulling speeds seem to indicate that this is not true for Gramicidin A. In this case, we have to consider the calculated diffusion coefficient a lower limit for the diffusivity of the pore.

B. Shape of the free energy profile

The free energy barrier for gA in Figure 4 is tent-shaped, so that the K^+ ion receives an average thermodynamic force in the outward direction. What produces

this specific shape is better understood by looking at the electrostatic force acting on the ion during translocation. We have computed the electrostatic potential between the ion and all the atoms within a sphere of radius 16 Å and 6 Å centered on the K^+ ion and averaged over the runs. The two distances are chosen in order to show the contributions of the first and second shells of atoms respectively. The electrostatic potential for the forward paths is shown in Figure 5a. The electrostatic profile produced by the first shell of atoms (dots in Figure 5a) corresponds to a potential energy gap of approximately 20 kcal/mol between the entrance ($z = -13$ Å) and the center ($z = 0$ Å) of the pore. The electrostatic energy barrier is however much higher (50 kcal/mol) and steeper for the larger interaction radius. The strong electrostatic contribution is due to the dipole formed by the bulk water molecules at the entrance of the pore which cannot be balanced by the apolar environment of the membrane surrounding the gA. While the potassium moves into the pore the lipids and the pore atoms are unable to polarize in the same way as the water molecules just outside the pore. In fact, at the center of the pore the first shell of atoms contributes to the entire electrostatic interaction energy with the ion as shown in Figure 5a which compares long and short ranged electrostatic interaction energy. Therefore, when the ion is pulled deeper into the pore, the contribution of polarized water diminishes until the first shell of atoms provides the entire electrostatic energy. The same considerations are valid in the reverse direction, Figure 5b, between the first and second shells showing that the potassium ion is embedded in a positive dipole which pushes it out of the pore (compare with the tent shaped free energy profile in Fig. 4).

Comparing the electrostatic potential between the forward and reverse pullings (Figure 5 a and b), it appears that the electrostatic barrier is higher for the forward run, however both cases reach the same value of the electrostatic interaction potential at the exit of the pore, indicating that the magnitude of the water molecule dipole is the same for the forward and reverse runs. The electrostatic energy difference comes almost entirely from the second shell of neighboring atoms around the ion which indicates the importance of the water dipole at the entrance of the pore. The non-equilibrium process in the forward run overestimate the energetic costs because the dipole moment is larger than it would be in the equilibrium situation as the water dipole moment did not have time to decay completely during the fast pulling. During the reverse runs, the dipole moment does not have the time to form until the ion is relative close to the pore entrance, thereby overestimating the outward energetic costs. In principle, the use of the Crooks fluctuation relation of Eq. 9 allows one to compute the equilibrium free energy from these non-equilibrium simulations in an exact manner. In practice, it is important that the bias, introduced by the accelerated dynamics along the reaction coordinate, is similar in the forward and reverse directions.

IV. DISCUSSION AND CONCLUSION

The tent shaped free energy profile for ion translocation through the gA pore originates from the different polarity of its inner part (including the atoms comprising the pore and the lipids surrounding it) with respect to bulk water. However, as pointed out by others, the fact that the gA pore can hold up to two potassium ions at a time has been seen as a consequence of the non-negligible polarity in the interior of the pore. Our results show to what extent the relatively lower polarity of the inner region of the gA pore creates a free energy barrier for ion crossing. The free energy barrier, along with the fact that the ions drag six to nine water molecules with them in a single file, makes gA a particularly challenging system for computer simulations, since short equilibrium simulations can mask what really occurs in the pore. In the current simulation studies we have assumed that the free energy profile is symmetrical with respect to the center of the pore. The free energy barrier from the entrance of the pore to the center can then be divided into three different regions. The first K^+ binding site at approximately -10 Å has been recognized by many different studies [49]. The second region from -10 Å to -5 Å is dependent on the interaction of the K^+ ion with the dipole moment generated by the water molecules outside the pore, while from -5 to zero the dipole is weaker and the molecular details of the binding with the oxygen atoms of the backbone of the pore itself become apparent.

The simulations presented here show an application of the new free energy reconstruction protocol proposed by Crooks[34], yielding similarly shaped free energy barriers for ion crossing to those reported in previous calculations [28]. The somewhat higher free energy barrier we have computed is possibly due to the failure to sample correctly the decay of the water dipole moment during the accelerated time of the simulation, whether this is based on pulling experiments or biased potentials (umbrella sampling). Also, the choice of initial conditions might play an important role due the state of the water dipole outside the pore. In fact, steered molecular dynamics accelerates the dynamics along the reaction coordinate (in this case z), but still requires the other degrees of freedom to equilibrate (for instance water molecules outside the pore). Furthermore, the use of periodic boundary conditions has been reported to be a non reliable method for the treatment of long range interactions for free energy calculations in charged and non-periodic systems (see [50] and references therein), even if special corrections were included. However, the current paper does not principally deal with the ability of PMF to reproduce free energy barriers for ion channels but it provides a sound alternative showing the potentiality of the reverse-forward method in simulating complex biological processes. Finally, the overestimation of the barrier for Gramicidin A has been suggested to be due to the electron polarizability which has not been included in the force field. This fact, already pointed out years ago

in a simulation of the gramicidin channel[51] has been noticed by preliminary tests in which a reduction of the barrier was obtained when smaller charges for the potassium ions were used. This reduction will be similar to that obtained using a simple polarizable force field, because of the global screening of electrostatic interactions by the induced field.

In this work we have presented one of the first applications of the Crooks fluctuation relation to ion channels. Our calculations reproduce with an extremely simple protocol the results for the free energy profile obtained previously and, more importantly, allow us to interpret the dynamic polarization of the water molecules outside the channel. The possibilities that the new formulation opens in computational biochemistry and biophysics are important, as it allows one to directly sample relevant regions of the phase space without the need to equilibrate in the direction of the reaction coordinate. This equilibration is still needed in the directions orthogonal to the given reaction coordinate, although the current protocol considerably simplifies the sampling problem by means of a more natural molecular simulation protocol. An additional advantage of the use of steered molecular dynamics is that it allows for the simultaneous evaluation of the PMF and the diffusion coefficient. The results of the non-equilibrium calculations presented here are of additional interest because they have been obtained with a limited number of trajectories (50) and total simulation time of just over 85 ns.

Finally, the computational protocol for forward-reverse steered molecular dynamics can fully exploit simple distributed network computing where many instances of the same simulation can be spawned on many independent machines volunteered by the general public [52]. This type of distributed infrastructure is not new but, so far,

it has not been possible to use it effectively for molecular dynamics simulations because of the limited computational power of each node (usually a PC) compared to the requirement of full-atom MD simulations [53]. However, recent advances in processor architectures and scientific software (CellMD [54]) have produced over an order of magnitude speed-up using the Sony-Toshiba-IBM Cell processor. By using the Cell processors available in the new Sony Playstation3, distributed computing initiatives such as PS3GRID.NET [55] can utilize a PS3 as effectively as a 20 core cluster and spawn computationally demanding jobs equivalent to the use of a higher end supercomputer for this specific application case. Such a scenario is of interest for SMD simulations because it allows one to leverage substantial computational power at considerably lower cost. We are currently using this infrastructure to investigate the same protocol starting with different initial conditions, different pulling speeds and spring strengths to study the effect of the distance from equilibrium in reconstructing the equilibrium free energy, as well as simple polarizability models in order to improve further the free energy profile obtainable.

Acknowledgments

GDF thanks HPC-Europa for a visiting grant and the Spanish Ramon y Cajal program. Partially funded by grant BQU2003-04448 (MCYT: Spanish Ministry of Science and Technology) and EC-STREP project QosCosGrid. The authors thankfully acknowledge the computer resources and assistance provided by the Barcelona Supercomputing Center and the use of the computer cluster Mavrino of the Centre for Computational Science in London.

-
- [1] F. M. Ashcroft, *Nature* **440**, 440 (2006).
 [2] M. T. Keating and M. C. Sanguinetti, *Cell* **104**, 569 (2001).
 [3] M. Grabe, H. C. Lai, M. Jain, Y. N. Jan, and L. Y. Jan, *Nature* **445**, 550 (2007).
 [4] C. H. Liu, T. Wang, M. Postma, A. G. Obukhov, C. Montell, and R. C. Hardie, *J Neurosci* **27**, 604 (2007).
 [5] F. Tombola, M. M. Pathak, P. Gorostiza, and E. Y. Isacoff, *Nature* **445**, 546 (2007).
 [6] V. B. Luzhkov and J. Åqvist, *Biochim Biophys Acta* **1747**, 109 (2005).
 [7] M. S. P. Sansom, I. H. Shrivastava, J. N. Bright, J. Tate, C. E. Capener, and P. C. Biggin, *Biochim Biophys Acta* **1565**, 294 (2002).
 [8] C. E. Capener, H. J. Kim, Y. Arinaminpathy, and M. S. P. Sansom, *Hum Mol Genet* **11**, 2425 (2002).
 [9] A. Giorgetti and P. Carloni, *Curr Opin Chem Biol* **7**, 150 (2003).
 [10] B. Roux, *Biophys. J.* **77**, 139 (1999).
 [11] D. P. Tieleman, P. C. Biggin, G. R. Smith, and M. S. Sansom, *Q Rev Biophys* **34**, 473 (2001).
 [12] S.-H. Chung, T. W. Allen, M. Hoyles, and S. Kuyucak, *Biophys J* **77**, 2517 (1999).
 [13] J. Åqvist and V. Luzhkov, *Nature* **404**, 881 (2000).
 [14] P. C. Biggin, G. R. Smith, I. Shrivastava, S. Choe, and M. S. Sansom, *Biochim Biophys Acta* **1510**, 1 (2001).
 [15] A. Burykin, M. Kato, and A. Warshel, *Proteins* **52**, 412 (2003).
 [16] A. Burykin, C. N. Schutz, J. Villà, and A. Warshel, *Proteins* **47**, 265 (2002).
 [17] B. Roux, T. Allen, S. Bernache, and W. Im, *Q Rev Biophys* **37**, 15 (2004).
 [18] M. Kato and A. Warshel, *J Phys Chem B Condens Matter Mater Surf Interfaces Biophys* **109**, 19516 (2005).
 [19] D. A. Doyle, J. Morais Cabral, R. A. Pfuetzner, A. Kuo, J. M. Gulbis, S. L. Cohen, B. T. Chait, and R. MacKinnon, *Science* **280**, 69 (1998).
 [20] G. Chang, R. H. Spencer, A. T. Lee, M. T. Barclay, and D. C. Rees, *Science* **282**, 2220 (1998).
 [21] J. Åqvist and A. Warshel, *Biophys J* **56**, 171 (1989).
 [22] B. Roux and M. Karplus, *Annu Rev Biophys Biomol Struct* **23**, 731 (1994).

- [23] G. V. Miloshevsky and P. C. Jordan, *Trends Neurosci* **27**, 308 (2004).
- [24] S. H. Chung and S. Kuyucak, *Biochim Biophys Acta* **1565**, 267 (2002).
- [25] A. B. Mamonov, R. D. Coalson, A. Nitzan, and M. G. Kurnikova, *Biophys J* **84**, 3646 (2003).
- [26] B. L. de Groot, D. P. Tieleman, P. Pohl, and H. Grubmüller, *Biophys J* **82**, 2934 (2002).
- [27] T. W. Allen, O. S. Andersen, and B. Roux, *Biophys. J.* **90**, 3447 (2006).
- [28] T. Bastug and S. Kuyucak, *J. Chem. Phys.* **126**, 105103 (2007).
- [29] S. Berneche and B. Roux, *Nature* **414**, 73 (2001).
- [30] B. Hille, *Ionic Channels of Excitable Membranes* (Sinauer Assoc. Inc., 1992).
- [31] G. Hummer and A. Szabo, *PNAS* **98**, 3658 (2001).
- [32] M. Jensen, S. Park, E. Tajkhorshid, and K. Schulten, *PNAS* **99**, 6731 (2002).
- [33] I. Kosztin, B. Barz, and L. Janosi, *J. Chem. Phys.* **124**, 064106 (2006).
- [34] G. E. Crooks, *Phys. Rev. E* **60**, 2721 (1999).
- [35] D. Frenkel and B. Smit, *Understanding molecular simulation* (Accademic Press, 1996).
- [36] C. H. Bennett, *J. Comput. Phys.* **22**, 245 (1976).
- [37] D. Collin, F. Ritort, C. Jarzynski, S. B. Smith, I. Tinoco, and C. Bustamante, *Nature* **437**, 231 (2005).
- [38] J. Choen, A. Arkhipov, R. Braun, and K. Schulten, *Biophys. J.* **91**, 1844 (2006).
- [39] G. De Fabritiis, J. Villà-Freixa, and P. V. Coveney, *Int J Mod Phys C* **in press** (2007).
- [40] C. Jarzynski, *Phys. Rev. Lett.* **78**, 2690 (1997).
- [41] K. S. Shing and K. E. Gubbins, *Mol. Phys.* **46**, 1109 (1982).
- [42] R. Delgado-Buscalioni, G. De Fabritiis, and P. V. Coveney, *Journal of Chemical Physics* **123**, 054105 (2005).
- [43] W. Humphrey, A. Dalke, and K. Schulten, *J. Molec. Graphics* **14**, 33 (1996).
- [44] A. MacKerell, D. Bashford, M. Bellott, R. Dunbrack, J. Evanseck, M. Field, S. Fischer, J. Gao, H. Guo, S. Ha, et al., *J. Phys. Chem. B* **102**, 3586 (1998).
- [45] J. C. Phillips, R. Braun, W. Wang, J. Gumbart, E. Tajkhorshid, E. Villa, C. Chipot, R. D. Skeel, L. Kalé, and K. Schulten, *J. Comp. Chem.* **26**, 1781 (2005).
- [46] T. Bastug and S. Kuyucak, *Eur. Biophys. J.* **34**, 377 (2005).
- [47] B. Roux, *Comp. Phys. Commun.* **91**, 275 (1995).
- [48] A. B. Mamonov, M. G. Kurnikova, and R. D. Coalson, *Biophys. Chem.* **124**, 268 (2006).
- [49] T. W. Allen, T. Bastug, S. Kuyucak, and S.-H. Chung, *Biophys. J* **84**, 2159 (2003).
- [50] A. Warshel, P. K. Sharma, M. Kato, and W. W. Parson, *Biochimica et Biophysica Acta* **1764**, 1641647 (2006).
- [51] J. Aqvist and A. Warshel, *Biophys. J.* **56**, 171 (1989).
- [52] Berkeley Open Infrastructure for Network Computing <http://www.boinc.berkeley.edu>.
- [53] S. Jha, M. Harvey, and P. Coveney, *Proceedings of ACM/IEEE SC 05* pp. 70–75 (2005).
- [54] G. De Fabritiis, *Comp. Phys. Comm.* **176**, 660 (2007).
- [55] PS3GRID project <http://www.ps3grid.net>.